

Molecular dynamics simulation of ethanol/water mixtures for structure and diffusion properties

Cuijuan Zhang, Xiaoning Yang*

Key Laboratory of Material-Orientated Chemical Engineering of Jiangsu Province, College of Chemistry and Chemical Engineering, Nanjing University of Technology, Nanjing 210009, PR China

Received 30 April 2004; received in revised form 1 March 2005; accepted 2 March 2005

Abstract

The structure and diffusion properties have been studied for ethanol/water mixtures at 298.15 K and atmospheric pressure by molecular dynamics (MD) simulation. The simulations were performed using a relatively simple rigid site–site model for ethanol and the TIP4P model for water. Partial radial distribution functions of pure water, pure ethanol and their binary mixtures are obtained to represent the microscopic structure properties. The self-diffusion coefficients and the mutual diffusion coefficients in the mixtures were calculated by the MD simulation. The self-diffusion coefficients of water and ethanol in the mixture are in qualitative agreement with the experimental data. The diffusion behavior of water in the aqueous solution is ascribed to the contributions of the “bound” water and the “free” water. The mutual diffusion coefficients keep fairly agreement with the experimental data. The effect of the distinct diffusion coefficient to the mutual diffusion coefficient has been evaluated and discussed. The simulation results suggest that the interaction potential models used is effective to describe the properties of the binary mixture.

© 2005 Elsevier B.V. All rights reserved.

Keywords: Molecular dynamics simulation; Water; Ethanol; Diffusion coefficient; Radial distribution function

1. Introduction

Alcohol is soluble in water by forming the hydrogen bonding with water, which makes the structure of the binary mixture more complicated [1,2]. An alcohol/water mixture often shows quite different properties from those observed for the corresponding pure components. Of particular interest are the structure and diffusion properties, which play important roles in the theoretical study and technological application involving mass transfer. At present, the aqueous solutions of alcohol are studied extensively by a variety of experimental techniques including dielectric relaxation [3], dynamic light scattering [4], NMR measurement [5], however, the physical–chemical behaviors and properties in the aqueous solutions have not yet been completely understood [6].

Although much effort has been made to study and predict the self-diffusion property in solutions through molecular dynamics (MD) simulation, only limit reports are available for the mutual diffusion coefficients by equilibrium molecular dynamics simulation. Compared with self-diffusion coefficient, mutual diffusion coefficient has much large uncertainty in its calculation because self-diffusion coefficient may be averaged over all particles of a given type while no such averaging is possible for mutual diffusion coefficients. Schoen and Hoheisel [7] studied the mutual diffusion coefficient for Ar/Kr model system by molecular dynamics simulation. Stoker and Rowley [8] calculated the mutual diffusion coefficient for selected alkanes in carbon tetrachloride using different combining rules for Lennard–Jones parameters. The mutual diffusion coefficient of methane/ethane mixture at high pressure was generated from the self-diffusion coefficients obtained by MD simulation using the Darken equation in the work of Keffer and Adhangale [9]. Castillo et al. [10] tried to understand the effect of molecular sizes and

* Corresponding author. Tel.: +86 2583587185; fax: +86 2583587185.
E-mail address: yangxia@njut.edu.cn (X. Yang).

interaction parameters on the concentration dependence of the mutual diffusion coefficients for Van der Waals binary mixtures. Zhou and Miller [11] compared the mutual diffusion coefficients of binary Ar/Kr mixtures by MD simulation to those from two empirical models: Darken's model and the common force model. In all the MD simulations above, the simple sphere Lennard–Jones model is adopted to represent these systems.

In addition, from a microscopic viewpoint, the knowledge of solution structure behavior is very fundamental to understand and elucidate the mixture diffusion phenomenon. Molecular dynamics simulation is a powerful tool in investigating the structure properties of solutions at a molecular level and it has been used widely to study the aqueous solutions [12,13]. However, most of previous reports [1,12,14–16] focused attention on the aqueous solutions of methanol and butyl alcohol. To our knowledge, few researches have been reported in literatures on the structure and diffusion properties, especially mutual diffusion coefficients, of the non-ideal ethanol/water mixture by molecular dynamics simulation.

Intermolecular potential functions are very crucial in a correct description of fluid properties by molecular simulation. The PIPF (a polarizable intermolecular potential function) force field has been developed to represent the ethanol molecule by Gao et al. [17] and the polarization effects are found to be significant in all alcohol liquids. Dynamic properties of supercooled ethanol have been studied by Sesé and Palomar [18]. Nevertheless, the development of the polarizable intermolecular potential function for condensed phase advances slowly. Hawlicka and Swiatla-Wojcik [19] studied the self-diffusion coefficients of water and methanol in NaCl–methanol–water systems using flexible potential models. To pure liquid alcohols, the OPLS force field developed by Jorgensen [20] has been applied to simulate the thermodynamics properties of alcohols. Recently, the dynamic properties of alcohol/water mixtures were calculated by MD simulation [21], in which the OPLS model was used for short alcohols and the TIP4P model was for water. The comparison between the MD results and the experimental data is only qualitatively satisfied. Furthermore, the structure behaviors in the solutions were not reported in the study [21]. Van Leeuwen [22] tested the applicability of a site–site interaction potential based on the OPLS model for pure alkanols by a MC simulation and quite satisfactory results of the vapor–liquid coexistence for pure ethanol were obtained in his work. Gotlib and Piotrovskaya [23] simulated the phase equilibrium and density of the binary ethanol–ethane mixture by combining the OPLS-based model of ethanol with a diatomic Lennard–Jones ethane model and the Lorentz–Berthelot mixing rules were adopted in the mixture simulation, consequently, an agreement between the experimental and simulated values was also obtained in their work.

In this work, the structure behaviors and diffusion properties for the ethanol/water solution are studied and the concentration dependence of the properties is investigated. In the

simulation, we apply a relatively simplified potential model based on the work of Van Leeuwen [22] to describe the ethanol molecule. To the water molecule, we adopt the TIP4P model. The Lorentz–Berthelot mixing rules are applied for the mixture parameters. In the following section we introduce the potential models and simulation details in this study. The radial distribution functions are presented to explain the structure behaviors in the solution. The results and discussions about the self-diffusion coefficients and the mutual diffusion coefficients in the ethanol/water mixtures are also showed in this section. Finally, conclusions and references are provided.

2. Theoretical approach

2.1. Potential model

In the simulation, the TIP4P [24,25] model is applied for the water molecule. The ethanol molecule is considered to be rigid structure which includes four interaction sites (methyl group, methylene group, oxygen atom and hydrogen atom). In the molecular model of ethanol, the bond angles of $\text{CH}_3\text{--CH}_2\text{--O}$ and $\text{CH}_2\text{--O--H}$ are 108° and 108.5° , respectively. The relevant bond lengths are listed in Table 1. The simplified rigid site–site model is adopted according to the simulation by Gotlib and Piotrovskaya [23] and Van Leeuwen [22]. However, for simplicity, the dihedral angle between the $\text{CH}_3\text{--CH}_2\text{--O}$ and $\text{CH}_2\text{--O--H}$ planes is considered to be a constant and only the trans configuration for ethanol molecules is considered in the simulation [26]. Thus, the torsional energy caused by the dihedral angle is zero in our simulation.

The intermolecular interaction between site i and site j is given by the Lennard–Jones potential and the Coulomb contribution

$$U_{ij}(r_{ij}) = 4\varepsilon_{ij} \left(\left(\frac{\sigma_{ij}}{r_{ij}} \right)^{12} - \left(\frac{\sigma_{ij}}{r_{ij}} \right)^6 \right) + \frac{q_i q_j}{r_{ij}} \quad (1)$$

where σ_{ij} is the size parameter, ε_{ij} the energy parameter, q_i the charge of site i and r_{ij} the distance between sites i and j . The values of Lennard–Jones parameters and the Coulomb charges used are given in Table 2, which are from Ref. [23]. Instead of the standard combining rules for OPLS model [27,28], the Lorentz–Berthelot rules are used for the interactions between different sites or atoms: $\sigma_{ij} = (\sigma_i + \sigma_j)/2$ and $\varepsilon_{ij} = \sqrt{\varepsilon_i \varepsilon_j}$.

The self-diffusion coefficients are calculated by both the Green–Kubo method (velocity autocorrelation function,

Table 1
Bond lengths in ethanol [23] and water [24] molecules

Bond	L (Å)
$\text{CH}_3\text{--CH}_2$ (ethanol)	1.53
$\text{CH}_2\text{--O}$ (ethanol)	1.43
O--H (ethanol)	0.945
O--H (water)	0.957

Table 2

Intermolecular Lennard–Jones parameters and Coulomb point charges for ethanol [23] and water [24] molecules

Group	ε/k (K)	σ (Å)	q (e)
CH ₃ (ethanol)	88.06	3.905	
CH ₂ (ethanol)	59.38	3.905	0.265
O (ethanol)	85.55	3.07	−0.700
H (ethanol)			0.435
O (water)	78.02	3.15	
H (water)			0.52
M (water)			−1.04

VACF) and the Einstein method (mean square displacement, MSD) [8,29]:

$$D_i = \frac{1}{3} \int_0^\infty \langle v_i(t_0) v_i(t_0 + t) \rangle dt \quad (2)$$

$$D_i = \frac{1}{6} \lim_{t \rightarrow \infty} \frac{d}{dt} \langle [r_i(t_0) - r_i(t_0 + t)]^2 \rangle \quad (3)$$

where $v_i(t)$ is the velocity of the center of mass of molecule i at time t , $r_i(t)$ the position of the center of mass of molecule i at time t .

The corresponding relationships for mutual diffusion coefficient are calculated by [8,30]:

$$D_{ij} = Q D_{ij}^0 = Q \int_0^\infty C(t) dt \quad (4)$$

where D_{ij}^0 is the kinetic mutual diffusion coefficient and $C(t)$ the relative velocity correlation function (RVCF) defined as

$$C(t) = \frac{1}{3N c_i c_j} \langle J_{ij}(t_0) J_{ij}(t_0 + t) \rangle \quad (5)$$

$J_{ij}(t)$ is a collective dynamical variable and Q is the thermodynamics factor. They are given as

$$J_{ij}(t) = c_j \sum_{k=1}^{N_i} v_k(t) - c_i \sum_{m=1}^{N_j} v_m(t) \quad (6)$$

$$Q \equiv 1 + \left(\frac{\partial \ln \gamma_1}{\partial \ln x_1} \right)_{T,P} \quad (7)$$

where c_i is the number density of molecule i , N_i the number of molecule i , γ_i the activity coefficient of component i and x_i the mole fraction of component i .

2.2. Simulation details

In this work, molecular dynamics simulations of ethanol/water mixtures were performed in the standard NVT ensemble in a cubic simulation cell and the Nosé–Hoover algorithm [31,32] was employed to keep the desired temperature 298.15 K. The experimental density data of the mixture [33] at atmospheric pressure was as an input for the NVT molecular dynamics simulation. The number of total molecules is 500 in the simulation. Each molecule in the MD

system was treated as single rigid unit, for which the molecular motion involves the translation of center of mass and the rotation around center of mass [34]. The rotation of the rigid unit was described by the quaternion of orientation. The dynamical equations of the rigid unit were integrated using the Beeman algorithm [35]. The time step in the MD runs was 0.5 fs. The long-range Coulomb interactions were handled using the Ewald summation technique in three dimensions. The starting configurations were obtained by a random displacement of the particles in the simulation cell. The periodic boundary condition was applied and a spherical cut-off with half the size of the cubic cell was used to truncate the molecular interactions. Each simulation was run 5×10^5 time steps. Judging by the temperature and the total energies, the system reaches equilibrium after the first 10^5 steps. Then we collected the trajectory data from the rest production steps.

3. Results and discussions

At first, the validity of the simplified rigid ethanol model and the parameters used is verified by the calculation of the enthalpy of vaporization, ΔH_{vap} , for pure ethanol [17,21]. The simulation results for pure ethanol and pure water are compared to the experimental data and the reference MD values [21] in Table 3. An agreement is obtained between the simulated and experimental values for ΔH_{vap} in the MD simulation.

The excess heats of mixing ΔH_{mix} determined from the NVT simulation in this study, along with the experimental data [36] and the NPT simulation values in reference [21] are plotted in Fig. 1. Our NVT simulation results (fixed

Table 3

Enthalpy of vaporization, ΔH_{vap} , of the pure liquids at 298.15 K

Molecule	ΔH_{vap} (kJ/mol)		
	MD		Experiment [21]
	This work	Ref. [21]	
Water	44.03 ± 0.31	43.86 ± 0.01	43.99
Ethanol	42.52 ± 0.38	41.43 ± 0.02	42.3

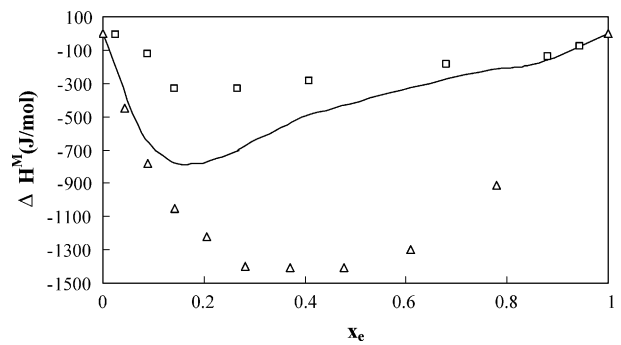


Fig. 1. Excess heat of mixing as a function of ethanol mole fraction in ethanol/water mixture. Solid line: experimental data [36]; (□) MD results in this study; (Δ) reference data [21].

experimental density) are overestimated at low ethanol concentration and are appropriate under high ethanol concentration. However, the mixing heats in Ref. [21] using NPT simulations (under atmospheric pressure) are noticeably underestimated except at very low ethanol concentration, in which the OPLS model is applied for the ethanol molecule and the TIP4P model for water molecule.

In order to further evaluate the rigid model, the pure ethanol MD at 298.15 K and atmospheric pressure were performed in NVT and NPT simulations by using both a flexible model, which uses our model parameters and includes the torsion interaction, and the rigid model. The time step is 1 fs and the total simulation duration is 1 ns. For the RDFs of O–H and O–O, there is no obvious difference between the flexible model and the rigid model. In the NPT run using the flexible model, the simulated density is 0.73 g/cm^3 and the obtained self-diffusion coefficient is $1.45 \times 10^{-9} \text{ m}^2 \text{ s}^{-1}$, which is identical to the reference data [21]; using the rigid model, the obtained self-diffusion coefficient is $1.24 \times 10^{-9} \text{ m}^2 \text{ s}^{-1}$ with the simulated density being 0.76 g/cm^3 , which is slightly better than the results from the flexible model. In the NVT run, the self-diffusion coefficient using the flexible ethanol model is $1.0 \times 10^{-9} \text{ m}^2 \text{ s}^{-1}$ with a simulated pressure being 183.2 bar, while using the rigid model results in $0.98 \times 10^{-9} \text{ m}^2 \text{ s}^{-1}$ with the simulated pressure 23.4 bar. Therefore, using the flexible model in NVT simulation under the experimental density also yields a reasonable diffusion coefficient. According to the above results, under the same ensemble condition (NPT or NVT), there is no obvious difference in the self-diffusion coefficient of pure ethanol between the flexible model and the rigid model. Thus, the effect of torsion interaction is small and, at least, the rigid model possesses an equivalent performance to the flexible model for the pure ethanol system. In summary, the rigid model for ethanol molecule should be acceptable in the following NVT MD simulation.

3.1. Structure properties

The radial distribution functions of ethanol/water mixtures at a series of concentrations have been obtained through the MD simulation. Figs. 2 and 3 illustrate the relevant O–H RDF in the solutions. According to the results, it appears that the concentration does not affect the positions of the peaks and the valleys in the RDFs but only their heights and depths. The corresponding coordination numbers ($N_c(r)$), determined by integration of the pair radial distribution functions, are plotted in the insets of Figs. 2 and 3. The O–H coordination number up to first valleys (around 2.5 \AA) is associated with the hydrogen bonding information in the mixtures [37]. The O–O RDFs are shown in Fig. 4 and the relevant O–O coordination numbers are given in the insets of Fig. 4. The O–O RDFs have maximum peaks at around 2.8 \AA for different concentrations. In contrast to the O–H RDFs, the second peak of the O–O RDFs with the position around $4.3\text{--}4.8 \text{ \AA}$ are not very obvious, indicating that there exists a weak second cor-

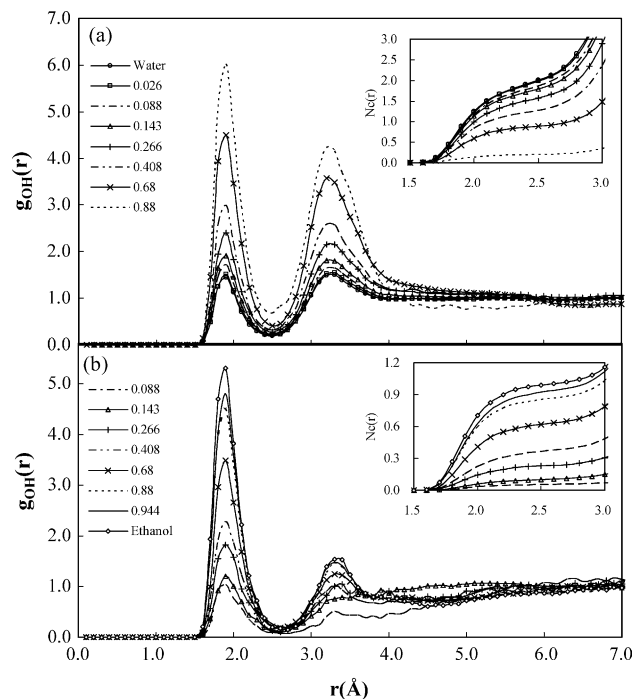


Fig. 2. O–H partial radial distribution functions for different mole fractions in ethanol/water mixture: (a) g_{OH} for water–water; (b) g_{OH} for ethanol–ethanol.

relation. The pair radial distribution functions of pure water are in good agreement with those from previous molecular simulations [1,25,38–40]. For pure ethanol, the radial distribution function in this work is also identical with the reference

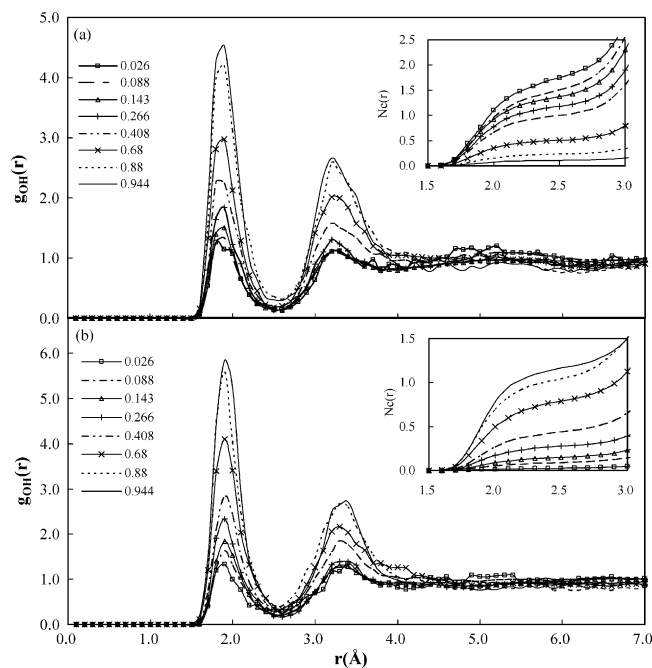


Fig. 3. O–H partial radial distribution functions for different mole fractions in ethanol/water mixture: (a) g_{OH} for ethanol–water; (b) g_{OH} for water–ethanol.

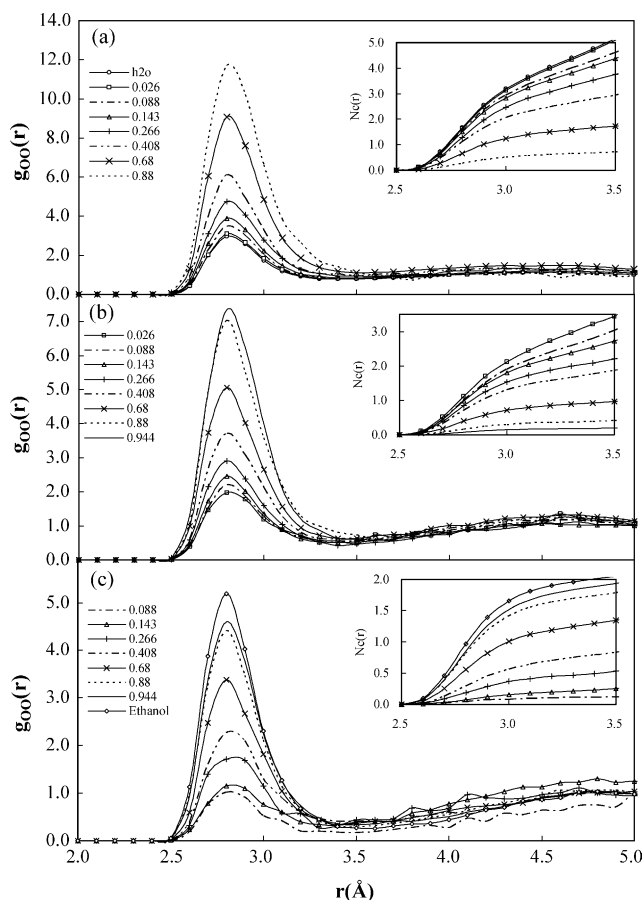


Fig. 4. O—O partial radial distribution functions for different mole fractions in ethanol/water mixture: (a) g_{OO} for water–water; (b) g_{OO} for ethanol–water; (c) g_{OO} for ethanol–ethanol.

reports [17,20,41,42] both in the positions and in the heights of peaks.

Water–water correlation. The large first peaks in the RDFs of Figs. 2(a) and 4(a) suggest that an obvious local water structure is in existence in the mixtures. For the highest concentration of ethanol, $x_e = 0.944$ studied, the RDF of water–water appears rather featureless and is omitted in the illustration. For the water–water structure, the coordination numbers of the water molecules in the first hydration shell of a given water molecule (up to 3.5 Å for O—O pair) decreases from 5 in pure water to 0.6 in the solution $x_e = 0.880$. This changing behavior agrees with a recent report for the aqueous solution of methanol [37]. Moreover, the O—H coordination numbers of water–water correlation, given in the insets of Fig. 2(a), also decrease as the ethanol concentration increases.

The first peak heights in the O—O RDF of water–water correlation are plotted against the mole fraction of ethanol in Fig. 5. The monotonic increase of the first peak height below $x_e = 0.880$ suggests the enhancement of local water structure due to the presence of the ethanol molecules. Within the ranges from low to intermediate ethanol concentrations, there exists sufficient water in the mixture system to keep the

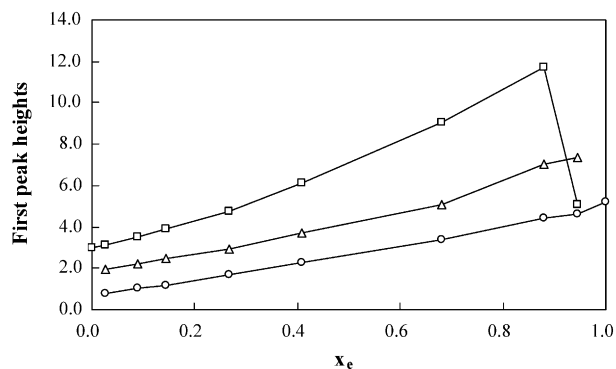


Fig. 5. Composition dependence of the first peak heights in the O—O radial distribution functions. The line is aided to eye: (□) water–water; (△) water–ethanol; (○) ethanol–ethanol.

local water structure. On the contrary, for very high ethanol concentration above $x_e = 0.880$, we can observe that the peak decreases drastically, as can be seen in Fig. 5. Under very dilute concentration of water, the water cluster structure becomes nonexistent in the mixture even if water still prefers to form clusters. This observation in Fig. 5 is consistent with the work of Ferrario et al. [14]. However, as stated by Laaksonen et al. [1], this strange behavior of the first peak height in the O—O RDF of water correlation could be due to inadequate simulation sampling at this high concentration point. Further extensive study is necessary.

The behaviors of hydrated water–ethanol molecules and local cluster of water molecules are pictorially represented in Fig. 6 by the representative snapshot (using the VMD visualization software) of a simulation trajectory, in which we

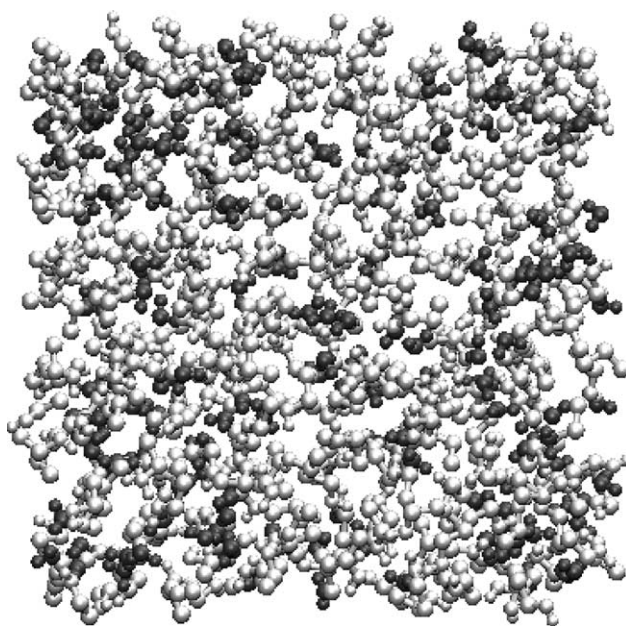


Fig. 6. A typical snapshot of the molecular dynamics simulation for ethanol/water mixture corresponding to the mole fraction of ethanol 0.680. Black color represents the water molecule and white color represents the ethanol molecule.

can visualize a typical equilibrium structure of the mixture. The snapshot shows that water and ethanol molecules are not randomly distributed and most of the water molecules exist as small cluster in the solution and rare water molecules show to be isolated. These results and analyses confirm again that the water structure can exist in a relatively concentrated alcohol–water solution [37].

Ethanol–ethanol correlation. For the ethanol structure in Figs. 2(b), 4(c) and 5, the amplitudes of the first maximum peaks in the O–H RDFs and the O–O RDFs increase with the addition of ethanol molecule. For the lowest concentration $x_e = 0.026$ studied, the RDF also appears rather featureless and it is not shown. The corresponding coordination numbers of ethanol–ethanol reduce from the ethanol-rich region to the water-rich region in the mixture. It implies that the ethanol–ethanol hydrogen bonding structure is gradually broken as the increase of water concentration. This picture might be interpreted as the fact that at the water-rich region the ethanol molecules have almost been hydrated by water molecules.

Ethanol–water correlation. The O–H and O–O RDFs for the ethanol–water correlation are presented in Figs. 3, 4(b) and 5. It is observed that the first peak becomes higher with the ethanol concentration increasing. The strong interaction between ethanol and water can result in an enhanced ethanol–water structure. As shown in the inserts of Figs. 3(a) and 4(b), for low ethanol concentration the coordination number of water hydrogen atoms per ethanol oxygen atom in separation <2.5 Å (O–H pair of ethanol–water correlation) is about one, and the coordination number of water oxygen atoms per ethanol oxygen atom with distance <3.5 Å is approximate three. At very high ethanol concentration, these coordination numbers reduce significantly due to not enough water molecules in the systems.

3.2. Self-diffusion coefficients

Fig. 7(a) shows the self-diffusion coefficients of water (D_w) in the mixtures obtained by two kinds of methods, mean square displacement (MSD) and velocity auto-correlation function (VACF). The experimental data [6] and the previous MD results [21] are also shown for comparison. Our simulation results are larger than the experimental data while lower than the MD values in Ref. [21]. The self-diffusion coefficients of ethanol (D_e) in mixtures are given in Fig. 7(b) together with the reference MD results [21] and the experimental data [43]. As discussed in the previous sections, the difference in the mixture self-diffusion coefficients between the rigid Van Leeuwen model and the OPLS model is probably due to the difference between NVT and NPT. It is observed that the self-diffusion coefficient of water or ethanol from MD simulation undergoes a process that it first descends then reaches smoothness as the molar fraction of ethanol increases. The trend of the simulated self-diffusion coefficients agrees with that of the experimental data. The decrease in D_w and D_e at low mole fraction of ethanol indicates that an ob-

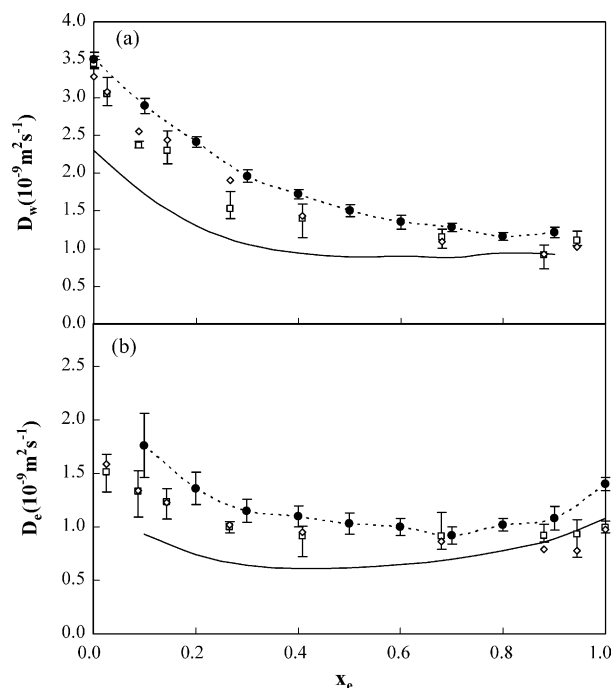


Fig. 7. (a) Self-diffusion coefficients of water in mixtures at 298.15 K. Only error bars of VACF results are shown for clarity: (\square) simulation values from VACF; (\diamond) simulation values from MSD; solid line: experimental data [6]; dashed line: MD results in Ref. [21]. (b) Self-diffusion coefficients of ethanol in mixtures at 298.15 K. Only error bars of VACF results are shown for clarity: (\square) simulation values from VACF; (\diamond) simulation values from MSD; solid line: experimental data [43]; dashed line: MD results in Ref. [21].

vious interaction between water and ethanol. This has been explained by the structure behaviors in the mixture. At higher concentrations of ethanol, the self-diffusion coefficients of water and ethanol are somewhat independent of the concentration with an analogous trend. This behavior corresponds to the situation that the movement between water and ethanol molecules is highly correlated in this concentration range. At very high ethanol concentration, water molecules lose its hydrogen bond network structure and behave as single molecule bonded with ethanol molecules by hydration.

The self-diffusion of water in mixture is usually described in terms of “bound” and “free” water molecules [44]. Follow the approach in the work of Bedrov et al. [44,45], the number of bound and free water molecules in the mixture can be counted by molecular simulation. Based on the O–O RDFs of ethanol–water correlation, the bound water is chosen as those being located within the first coordination shell of ethanol molecule. So the definition of bound water assumes that a water molecule is bound to an ethanol molecule if the distance between the water oxygen atom and the ethanol oxygen atom is below 3.5 Å. Fig. 8 gives the fraction (X_b) of bound water molecules, a ratio between the bound water number and the total water number, as a function of ethanol composition. As seen in Fig. 8, the fraction of bound water increases with the ethanol concentration increasing. For highly concentrated solution, most of water molecules are bound and the

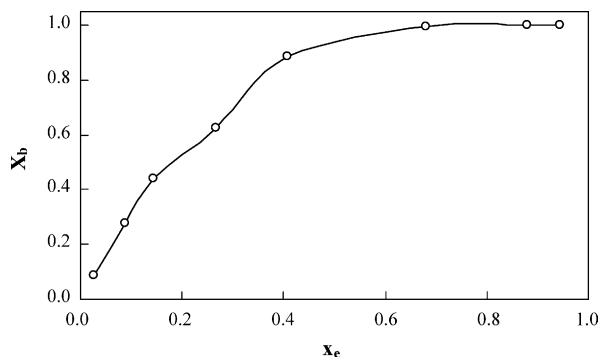


Fig. 8. Fraction of bound water calculated by the molecular dynamics simulation in ethanol/water mixture.

self-diffusion coefficients of water are intensively relevant to that of ethanol.

According to the analysis above, the self-diffusion of water in the ethanol/water solution can be represented as two contributions of the free water and the bound water as follows [44,45]:

$$D_w = (1 - X_b)D_w^0 + X_b K_b D_e \quad (8)$$

where D_w^0 is the diffusion coefficient of pure water, D_e the self-diffusion coefficients of ethanol in mixtures, X_b the obtained fraction of bound water and K_b the bound coefficient supposed to be greater than unity [44,45]. By fitting the obtained self-diffusion coefficients in the mixtures from the MD simulation (for clarity, only MSD results are shown) with Eq. (8), the parameter $K_b = 1.24$ is obtained. As shown in Fig. 9, Eq. (8) reasonably describes the concentration dependence of the self-diffusion coefficient of water in ethanol/water systems.

3.3. Mutual diffusion coefficients

In order to obtain mutual diffusion coefficients, the relative velocity correlation functions, $C(t)$ are calculated by Eq. (5). The oscillation of RVCF for the mixture is more significant than that of VACFs. The mutual diffusion coefficient (D_{we})

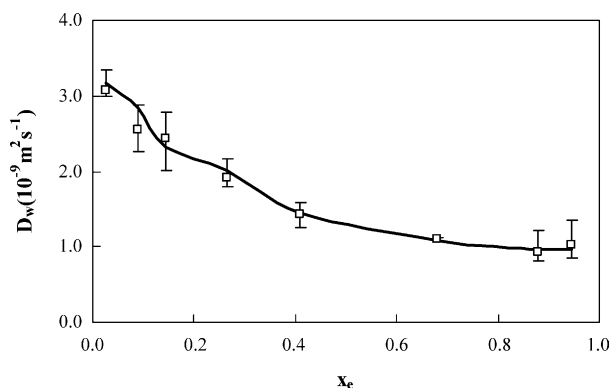


Fig. 9. Fitting results of Eq. (8) for self-diffusion coefficients of water as a function of ethanol concentration: (□) MD results in this study; solid line: the fitting results from Eq. (8).

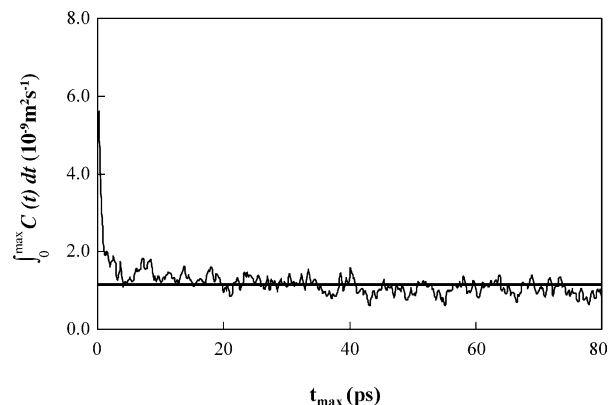


Fig. 10. The integral of RVCF $C(t)$ as a function of upper limit of integration time at the mole fraction of ethanol 0.408. The straight line is the average value.

calculated from RVCF possesses a relatively low accuracy, because RVCF is a collective quantity and shows large fluctuations in comparison to VACF [30]. A typical example of the integral of $C(t)$ is illustrated in Fig. 10 as a function of the upper limit of integration time (t_{\max}). As shown in this figure, the integral converges to a relatively defined value by about 10 ps. The curve fluctuates around a mean value beyond 10 ps and we discard the values below 10 ps. Thus, the integral value has been averaged over 10–75 ps.

In this work, a similar procedure is adopted in the calculations of the mutual diffusion coefficients in order to obtain reasonable results. The thermodynamic factor Q depends on the derivative of chemical potential with respect to composition. Although it can be computed from molecular simulation according to the Kirkwood-Buff theory [46], generally it is difficult to acquire good statistical results [47,48]. Here the value of Q is calculated from the vapor–liquid phase equilibrium data of ethanol/water [49,50]. The mutual diffusion coefficients calculated by Eq. (4) are plotted in Fig. 11 across the entire concentration range together with the experimental data [51]. Presently, there are relatively fewer research reports on the mutual diffusion coefficient of real mixtures from MD

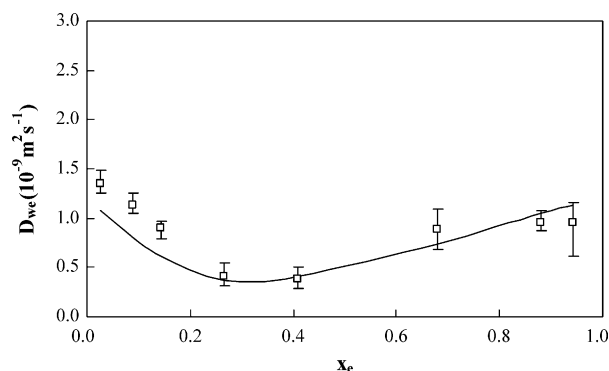


Fig. 11. Mutual diffusion coefficients (D_{we}) in the ethanol/water mixtures as a function of ethanol concentration. Solid line: experimental data [51]; (□) MD results in this work.

simulation possibly because of the inherently poor statistics in the calculation of the collective property. However, in this study a relatively acceptable agreement is obtained for the mutual diffusion coefficients of ethanol/water between the MD results and the experimental data [51].

Based on the linear response theory [11,30,46], the mutual diffusion coefficient of binary mixtures can be written as

$$D_{we} = D_s + D_d \quad (9)$$

$$D_s = Q(D_w x_e + D_e x_w) \quad (10)$$

$$D_d = Q x_w x_e [f_{ww} + f_{ee} - 2f_{we}] \quad (11)$$

where D_s is the Darken diffusion coefficient [11] and it depends on the component self-diffusion coefficients in mixture and D_d is defined as the distinct diffusion coefficient. The detailed theoretical description can be found elsewhere [11,30]. The f_{ww} , f_{ee} and f_{we} represent the cross velocity correlations of two different particles for the same or different species in mixtures [46] and they can be related to specific interactions between molecules.

The velocity cross-correlation functions can be evaluated through the kinetics mutual diffusion coefficients and the self-diffusion coefficients in mixtures as follows [46,52]:

$$f_{ij} = -\frac{D_{ij}^0 M_i M_j}{(x_i M_i + x_j M_j)^2}, \quad i \neq j \quad (12)$$

$$f_{ii} = \left[-D_i + \frac{D_{ij}^0 M_j^2 x_j}{(x_i M_i + x_j M_j)^2} \right] \frac{1}{x_i}. \quad (13)$$

Fig. 12(a) gives the concentration dependence of the three cross-correlation functions (f_{ee} , f_{ww} , and f_{we}) obtained from Eqs. (12) and (13), where the kinetic mutual diffusion coefficients and the relevant self-diffusion coefficients are taken from the previous molecular dynamics simulations. It can be observed that f_{ww} goes firstly from negative to positive values with mole fraction of ethanol increasing and then it reaches a maximum value. This behavior of f_{ww} suggests that the addition of ethanol will enhance the water–water correlation and this correlation will become weak beyond a high ethanol concentration. This result is consistent with the analysis of the radial distribution function for the water–water correlation in the preceding section. The negative behavior of f_{ee} implies that the relatively weak correlation between ethanol molecules as compared with the water species. An expected negative value [11] is obtained for f_{we} , which lies between the values of f_{ee} and f_{ww} . The decreasing negativity of f_{we} indicates again the strengthening of water–ethanol correlation (or cluster) with the ethanol concentration increasing.

In order to further evaluate the contribution from the distinct diffusion to the mutual diffusion, a ratio R is defined as [30]

$$R = \frac{D_{we}}{D_s} = \frac{D_{we}^0}{x_w D_w + x_e D_e} \quad (14)$$

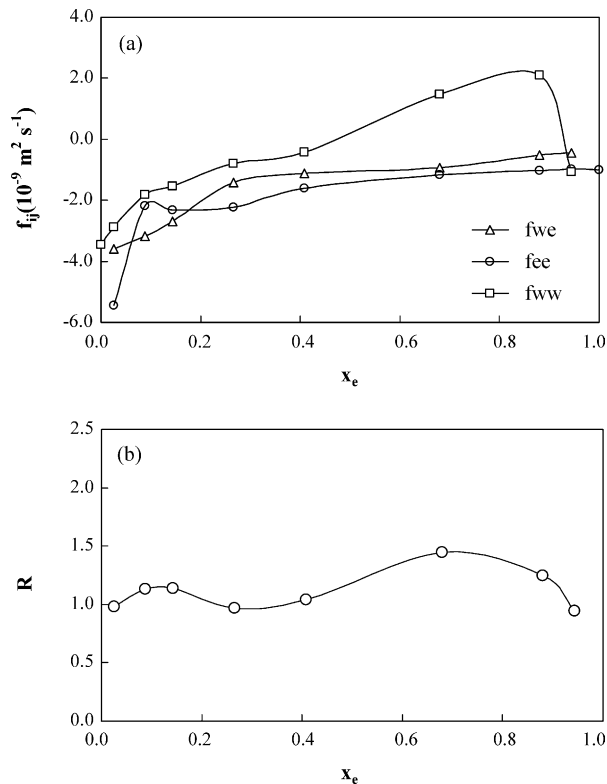


Fig. 12. (a) Velocity cross-correlation functions in ethanol/water mixture evaluated from Eqs. (12) and (13). (b) The ratio R as a function of ethanol concentration.

This definition (R) eliminates the effect owing to the thermodynamics non-ideality of mixture. In the previous study [53], both positive and negative contributions from distinct diffusion to mutual diffusion in different mixture systems were observed. When $R > 1$ (D_d is positive) the distinct diffusion enhances the mutual diffusivity. If $R < 1$ (D_d is negative) the distinct diffusion retards the mutual diffusivity. For ethanol/water mixture, R is plotted in Fig. 12(b) as a function of solution concentration. It is shown that the effects of the distinct diffusion on the mutual diffusion in water/ethanol mixtures are quite complicated. Under low and medium ethanol concentrations, the values of R fluctuate around unity, which means the distinct diffusion has relatively little effect on the mutual diffusion. As suggested before [46,52], the positive contribution means that the velocity correlations between the same species are much stronger than those between different species, and the same species molecules have more tendency to diffuse together, while the negative D_d hints that the different species molecules have more tendency to diffuse together. It is notable that the highest R ($R = 1.44$) appears around $x_e = 0.680$, which is an index of strong correlation (cluster) at this composition. The distinct diffusion coefficient is determined by the three cross velocity correlation functions, thus, the large positive contribution from the distinct diffusion to the mutual diffusion is mainly attributed to the strong water–water correlation in the mixture.

4. Conclusions

In this study, molecular dynamics simulations are performed for the ethanol/water mixture to study the structural and dynamical properties of the mixtures. In the simulation, a site–site rigid model is applied for ethanol molecule and the TIP4P model for water molecule.

Then O–O and O–H RDFs are obtained to study the local structure in the binary mixture covering the entire concentration range. From the RDFs and the relevant coordination numbers, we find that water–water correlation is enhanced in the mixtures compared to that in pure water, while the ethanol–ethanol hydrogen bonding structure is gradually broken as the water concentration increases. For the ethanol–water correlation the strong interaction between ethanol and water molecules leads to an enhancement in the ethanol–water structure with ethanol concentration increasing.

The self-diffusion coefficients of water and ethanol under different concentrations are compared with the MD result in the reference and the experimental data. Our simulation values are larger than the experimental data but smaller than the reference MD results. The concentration dependence of the self-diffusion coefficients is related to the structure behavior of the mixture. In the aqueous solution, the self-diffusion coefficient of water is described by the combining contribution of the “bound” and “free” water molecules. The mutual diffusion coefficients obtained from the MD simulation are in fair agreement with the experimental data in the ethanol/water mixture. The velocity cross-correlation functions are evaluated in terms of the kinetics mutual diffusion coefficient and self-diffusion coefficients from the simulation. The distinct diffusion coefficient possesses an obvious effect upon the mutual diffusion coefficient. This effect can be ascribed as the strong water–water correlation in the solution. Finally, it is shown that the combination between the ethanol and water models is viable for representation of the structure and diffusion properties of the ethanol/water mixture.

Acknowledgement

This work was supported by the National Natural Science Foundation of China through Grant No. 20276028 and by the Research Grant 02KJB530002 from Jiangsu Provincial Committee of Education in China. The starting research funding of overseas scholar from Ministry of Education of China is greatly acknowledged.

List of symbols

c_i	number density of molecule i
$C(t)$	relative velocity correlation function (RVCF) at time t
D_d	distinct diffusion coefficient
D_i	self-diffusion coefficient of species i

D_{ij}	mutual diffusion coefficient of binary mixture of i and j
D_s	the Darken diffusion coefficient in Eq. (10)
f_{ij}	the cross velocity correlations between different particles of the same species ($i=j$) or different species ($i \neq j$) in mixtures
$g(r)$	radial distribution functions
K_b	bound coefficient
M_i	molar mass of species i
$N_c(r)$	coordination numbers around atom or site
N_i	total number of molecule i
q_i	charge of group or atom i
Q	thermodynamic factor
$r_i(t)$	position of molecule i at time t
r_{ij}	the distance between sites i and j
$v_i(t)$	velocity of molecule i at time t
x_i	mole fractions of component i in mixtures
X_b	fraction of bound water in mixtures

Greek letters

γ_i	activity coefficient of component i
ε	the energy parameter of Lennard–Jones potential
σ	the size parameter of Lennard–Jones potential

Subscripts

w	water species
e	ethanol species

References

- [1] A. Laaksonen, P.G. Kusalik, I.M. Svishchev, J. Phys. Chem. A 101 (1997) 5910–5918.
- [2] E. Guàrdia, J. Martí, J.A. Padró, L. Saiz, A.V. Komolkin, J. Mol. Liquid 96–97 (2002) 3–17.
- [3] P. Petong, R. Pottel, U. Kaatz, J. Phys. Chem. A 104 (2000) 7420–7428.
- [4] K. Iwasakaki, T. Fujiyama, J. Phys. Chem. 81 (1977) 1908–1912.
- [5] K.R. Harris, P.J. Newitt, J. Phys. Chem. B 102 (1998) 8874–8879.
- [6] W.S. Price, H. Ide, Y. Arata, J. Phys. Chem. A 107 (2003) 4784–4789.
- [7] M. Schoen, C. Hoheisel, Mol. Phys. 52 (1984) 33–56.
- [8] J.M. Stoker, R.L. Rowley, J. Chem. Phys. 91 (1989) 3670–3676.
- [9] D.J. Keffer, P. Adhangale, Chem. Eng. J. 100 (2004) 51–69.
- [10] R. Castillo, C. Garza, H. Dominguez, J. Chem. Phys. 100 (1994) 6649–6657.
- [11] Y. Zhou, G.H. Miller, Phys. Rev. E 53 (1996) 1587–1601.
- [12] P.G. Kusalik, A.P. Lyubartsev, D.L. Bergman, A. Laaksonen, J. Phys. Chem. B 104 (2000) 9533–9539.
- [13] A.K. Soper, J.L. Finney, Phys. Rev. Lett. 71 (1993) 4346–4350.
- [14] M. Ferrario, M. Haughney, I.R. McDonald, M.L. Klein, J. Chem. Phys. 93 (1990) 5156–5166.
- [15] J.T. Slusher, Fluid Phase Equilib. 154 (1999) 181–192.
- [16] J.M. Stubbs, B. Chen, J.J. Potoff, J.I. Siepmann, Fluid Phase Equilib. 183–184 (2001) 301–309.
- [17] J. Gao, D. Habibollazadeh, L. Shao, J. Phys. Chem. 99 (1995) 16460–16467.
- [18] G. Sesé, R. Palomar, J. Chem. Phys. 114 (2001) 9975–9981.
- [19] E. Hawlicka, D. Swiatla-Wojcik, Phys. Chem. Chem. Phys. 2 (2000) 3175–3180.
- [20] W.L. Jorgensen, J. Phys. Chem. 90 (1986) 1276–1284.

- [21] E.J.W. Wenisnk, A.C. Hoffmann, P.J. van Maaren, D. van der Spoel, *J. Chem. Phys.* 119 (2003) 7308–7317.
- [22] M.E. Van Leeuwen, *Mol. Phys.* 87 (1996) 87–101.
- [23] I.Yu. Gotlib, E.M. Piotrovskaya, *J. Phys. Chem. B* 103 (1999) 7681–7686.
- [24] W.L. Jorgensen, J. Chandrasekhar, J.D. Madura, R.W. Impey, M.L. Klein, *J. Chem. Phys.* 79 (1983) 926–935.
- [25] A.A. Chialvo, P.T. Cummings, *J. Phys. Chem.* 100 (1996) 1309–1316.
- [26] B. Kvamme, *Fluid Phase Equilib.* 131 (1997) 1–20.
- [27] W.L. Jorgensen, C.J. Swenson, *J. Am. Chem. Soc.* 107 (1985) 569–578.
- [28] W.L. Jorgensen, J.D. Madura, C.J. Swenson, *J. Am. Chem. Soc.* 106 (1984) 6638–6646.
- [29] Y. Zhou, G.H. Miller, *J. Phys. Chem.* 100 (1996) 5516–5524.
- [30] C.R. Kamala, K.G. Ayappa, S. Yashonath, *Phys. Rev. E* 65 (2002) 061202.
- [31] S. Nosé, *Mol. Phys.* 52 (1984) 255–268.
- [32] W.G. Hoover, *Phys. Rev. A* 31 (1985) 1695–1697.
- [33] E.W. Washburn, *International Critical Tables of Numerical Data, Physics, Chemistry and Technology*, Knovel, New York, 2003.
- [34] M.P. Allen, D.J. Tildesley, *Computer Simulation of Liquids*, Clarendon Press, Oxford, 1987.
- [35] D. Beeman, *J. Comp. Phys.* 20 (1976) 130–139.
- [36] J.A. Boyne, A.G. Williamson, *J. Chem. Eng. Data* 12 (1967) 318.
- [37] S. Dixit, J. Crain, W.C.K. Poon, J.L. Finney, A.K. Soper, *Nature* 416 (2002) 829–832.
- [38] S. Okazaki, K. Nakanishi, H. Touhara, *J. Chem. Phys.* 78 (1983) 454–469.
- [39] S. Okazaki, H. Touhara, K. Nakanishi, *J. Chem. Phys.* 81 (1984) 890–894.
- [40] D. Bedrov, O. Borodin, G.D. Smith, *J. Phys. Chem. B* 102 (1998) 5683–5690.
- [41] L. Saiz, J.A. Padró, E. Guàrdia, *J. Phys. Chem. B* 101 (1997) 78–86.
- [42] M.A. González, E. Enciso, F.J. Bermejo, M. Bée, *J. Chem. Phys.* 110 (1999) 8045–8059.
- [43] A.J. Easteal, L.A. Woolf, *J. Phys. Chem.* 89 (1985) 1066–1069.
- [44] D. Bedrov, O. Borodin, G.D. Smith, *J. Phys. Chem. B* 102 (1998) 9565–9570.
- [45] O. Borodin, D. Bedrov, G.D. Smith, *J. Phys. Chem. B* 106 (2002) 5194–5199.
- [46] T. Kato, *J. Phys. Chem.* 89 (1985) 5750–5755.
- [47] Y. Kataoka, *J. Mol. Liquid* 90 (2001) 35–43.
- [48] Y. Kataoka, *Fluid Phase Equilib.* 144 (1998) 257–267.
- [49] X.N. Yang, R.S. Wang, *Chin. J. Chem. Eng.* 4 (1996) 104–111.
- [50] J. Gmehling, U. Onken, *Vapor–Liquid Equilibrium Data Collection, Aqueous–Organic Systems, Chemistry Data Series, Part 1, vol. 1, DECHEMA*, 1977.
- [51] M.T. Tyn, W.F. Calus, *J. Chem. Eng. Data* 20 (1975) 310–316.
- [52] R. Mills, R. Malhotra, L.A. Woolf, D.G. Miller, *J. Phys. Chem.* 98 (1994) 5565–5575.
- [53] R. Sharma, K. Tankeshwar, *J. Chem. Phys.* 108 (1998) 2601–2607.